Influence of geometry and material properties on resonant frequencies and sensitivity of MEMS cantilever-type structures

G. IONAŞCU[a*], A. SANDU[b], E. MANEA[c], R. GAVRILA[c], C. D. COMEAGA[a], L. BOGATU[a], D. BESNEA[a]
[a]*Mechatronics and Precision Mechanics Department, "Politehnica" University of Bucharest, Romania*
[b]*Department of Strength of Materials, "Politehnica" University of Bucharest, Romania*
[c]*National Institute for Research & Development in Microtechnology of Bucharest, Romania*

The paper presents the analysis and simulation of three shapes of cantilevers – rectangular, triangular and trapezoidal with a rectangle tip (the two last ones of inner cut form), micromachined through Micro-Electro-Mechanical Systems (MEMS) technology. The vibration modes and the resonant (natural) frequencies were determined by Finite Element Method (FEM), and measured using Laser-Doppler Vibrometry (LDV) by scanning with the Polytec MSA–500 system, and also by Atomic Force Microscopy (AFM). Based on validated models of numerical computation, the sensitivity has been predicted for a chemical detection application. The influence of structural geometry (shape and sizes, measured by Scanning Electron Microscopy – SEM) and material properties (silicon Young's modulus, estimated with analytical expressions for the simplest shape cantilever – the rectangular one, and measured by nanoindentation) have been pointed out with respect to the dynamic behavior (analyzed from the perspective of resonant frequencies) and sensitivity of the analyzed MEMS structures.

(Received November 14, 2013; accepted May 15, 2014)

Keywords: MEMS cantilever, Resonant frequency, Young's modulus, FEM, LDV, AFM, SEM, Nanoindentation

1. Introduction

Microcantilevers are miniaturized mechanical structures widely encountered in MEMS devices (sensors and actuators). They can be built as single components or in arrays. The application of a cantilever determines its design, the used materials, the operating characteristics and the fabrication method. Applications that have enabled nanotechnology such as atomic force microscopy, chemical and biological particles detection, actuation for optical switching or micromanipulators, and, also, measurement of different mechanical properties of materials (Young's modulus, surface force/stress, mass loading, residual stress, internal friction of the material, the ageing process, and the effect of the operating environment) rely especially on microcantilevers [1-6].

Two basic types of operating schemes are employed, one of them involves deflection of the cantilever beam structure under a load or intrinsic stress applied/generated on/or within the cantilever in static condition, and the other one consists of the change in the resonant frequency of the cantilever beam structure due to the mass loading on the beam in dynamic condition. For example, this change is induced by the absorption of chemical species into a sensitive coating of the microcantilever used as chemical sensor. An accurate modal analysis makes possible to estimate the sensitivity of the cantilever or its ability to detect minimum frequencies shifts induced by the absorption of analyte. In order to obtain a high sensitivity, the structure must be designed so that its resonant frequency be high and its equivalent mass be small.

Thus, to improve the performance, many researchers have studied and developed various models for understanding cantilever behaviour [7-13]. Different geometries were analyzed (rectangle (conventional) or paddle shape cantilever, „V-shaped" microcantilevers with linear arms or a nonlinear width profile, cantilevers with full or inner cut rectangle/triangle/trapeze/half-ellipse shape, a.s.o.) and various materials were used (mono-/polycrystalline silicon, silicon-oxide, silicon-nitride or polymers like SU-8) and processed through bulk or surface micromachining (employing crystalline anisotropy property of a silicon wafer or sacrificial layer technique and, also, photolithography and etching processes). Recent developments combine the micromachining technologies specific to micromechanical components with the latest integrated circuit (IC) and complementary metal oxide semiconductor (CMOS) technologies to produce intelligent extremely small cantilevers.

In this paper, a new approach is proposed in order to increase the precision of the computation models for the simulation of micromechanical structures under study. The simplest configuration – a reference rectangular cantilever, made from silicon through bulk micromachining, is analyzed from experimental and theoretical point of view, using both analytical and numerical models, to validate the numerical computation models for the more complex shape cantilevers – triangular and trapezoidal with a rectangle tip, both of them of inner cut form and made

from silicon-oxide deposited on a silicon wafer used as sacrificial material, Fig. 1. The numerical computation was performed by FEM (isotropic, 3D and 2D models). Silicon Young's modulus, used in the FEM models, was initially estimated with analytical expressions for the rectangular cantilever, and then measured by nanoindentation. The vibration modes and the resonant (natural) frequencies were determined and compared with those measured by LDV method using MSA–500 system (Polytec) and, also, an atomic force microscope, Ntegra Scanning Probe Microscope (NT-MDT Co.). Finally, based on the validated models, and considering the computation models for non-homogeneous structures of the complex shape cantilevers coated with a palladium thin film, the natural frequencies and sensitivity have been predicted for a hydrogen detection application. Interesting conclusions regarding the influence of structural geometry and material properties on the dynamic behaviour and sensitivity of the analyzed MEMS structures have been inferred.

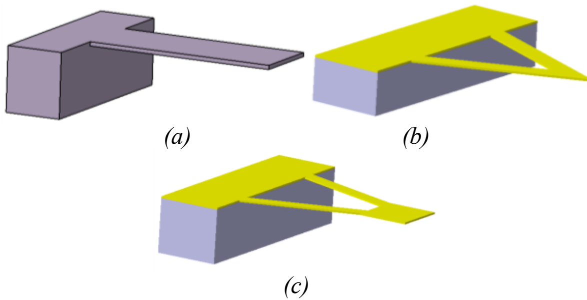

Fig. 1. 3D views of the analyzed cantilever structures: rectangular (a) – full form, triangular (b) and trapezoidal with rectangle tip (c) – inner cut forms.

2. Theoretical and experimental dynamic analysis of rectangular cantilever

Reference silicon microcantilevers have been used to validate the numerical computation. They are of conventional (rectangular) type, with constant width, Fig. 2, for which analytical computation expressions of the eigen (natural) frequencies can be found in the scientific literature.

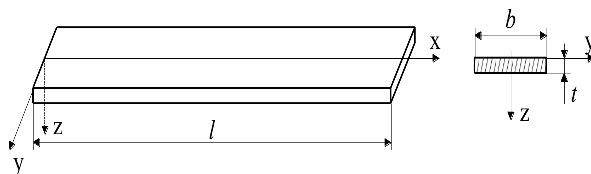

Fig. 2. Sketch of the rectangular microcantilever.

Two computation models were considered, using SolidWorks 2011/COSMOS M software.

The **model 1** (3D FEM) has employed meshing in three-dimensional elements with 8 nodes/element – **3D SOLID**; 20,000 elements interconnected in 25,755 nodes have resulted. This computation model can be used for non-homogeneous structures, too (composite structures, e.g. a film-substrate structure).

The **model 2** (2D FEM) has employed meshing in elements of thin plate with 3 nodes/element – **SHELL 3**; 4,000 elements interconnected in 2,121 nodes have resulted. This computation model can be used only for homogeneous and thin structures, made from a single material.

The microcantilever is a microbeam clamped at one end (with all degrees of freedom blocked) and with the other end suspended freely outwards.

In our study, the structure material is silicon, with a density of ρ_{Si} = 2330 kg/m^3. Among the mechanical properties of interest, one can be mentioned the elastic properties (Young's modulus (E) and Poisson's ratio) directly related to the device performance (mechanical behaviour). If for Poisson's ratio, the accepted value by the most of authors is ν_{Si} = 0.22, for E more values are used, as 98, 130, 150, 170 GPa, depending on certain factors, the most important being the fabrication technology of structure [14]. Considering these uncertainties, in a first estimation, the value of E has been established starting from the values of the resonant (natural) frequencies provided by the producer [15] and those computed with analytical expressions given in (1) – (3) [16]:

$$f_i = \frac{n_i^2}{2\pi l^2}\sqrt{\frac{EI_y}{\rho A}} \tag{1}$$

$$I_y = \frac{bt^3}{12} \tag{2}$$

$$A = b \cdot t \tag{3}$$

where: EI_y – the bending stiffness; I_y – the inertia moment of the cross section related to Oy axis; l, A – the length and cross-sectional area of the beam; b, t – the width and thickness of the beam; ρ – the density of the beam material; n_i – coefficients with specified values corresponding to the vibration modes. For the first three bending modes, values of n_i are the followings: n_1 = 1.875; n_2 = 4.694; n_3 = 7.855.

The values of E for different lengths of cantilever, computed with the equations from above, based on the resonant frequencies extracted from the producer's data sheet, are listed in Table 1.

Table 1. Values of Young's modulus (E).

Dimensions of microbeam			f_I (kHz), Data sheet	*E* (GPa), Analitically computed
b = 90 µm *t* = 5 µm	*l*, µm	500	~24.3	131.8
		750	~10.8	131.8
		1000	~6.1	132.8
Mean				132.1

Because the values of the resonant (natural) frequencies provided by the producer are average values, taking into account the dimensional differences, an accepted value of 130 GPa can be adopted for the silicon Young's modulus. Using this value for E, in Table 2 are given the values of the fundamental eigen frequency (f_1) computed analitically (with Eqn. (1)) and numerically (by FEM) for the cantilever of l=750 µm, as well as the experimentally determined value through LDV method by employing the MSA–500 Micro System Analyzer (Polytec), Fig. 3. The same value of 13.28 kHz was found for all the eight microbeams of the tested chips. The measurements were made on individual chips bonded onto a metal rigid plate of 12 x 12 x 5 mm^3. The plate was fixed through an elastic double adhesive layer on a piezoelectric excitator consisting of a multilayer ceramics piezoelectric actuator mounted in an elastic pre-tensioned housing.

In order to measure and to verify alternatively the first resonant frequency of the chip cantilevers, similar experiments were made on the atomic force microscope, Ntegra Scanning Probe Microscope, too. It was found 12.5 kHz on one chip, and 14.3 kHz, Fig. 4, on another chip (the average value of 13.4 being very close to that one measured with MSA–500).

Table 2. Values of the fundamental eigen frequency (f_1).

Method	f_1 (kHz)
Analitic	10,724
FEM, *model 1*	10,774
FEM, *model 2*	10,773
Experimental, MSA–500	13,28
Experimental, AFM	13.4

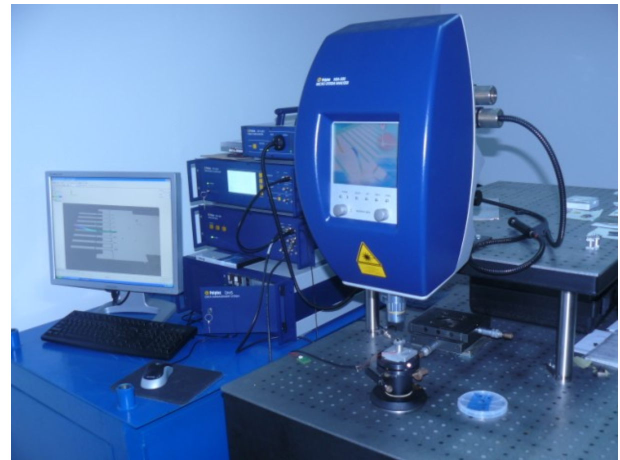

Fig. 3. The system of Polytec MSA-500, left (bottom to up): Data Management System, Vibrometer Controller, and Junction Box, right: Fiber-Optic Interferometer and Measurement Head. The tested structure can be viewed on the monitor screen.

It can observe that the results of the two models are practically identical, and very close to those obtained using the Eqn. (1). Because the second model is simpler than the first one, for homogeneous structures of complex geometry is useful that meshing be performed in elements of thin plate **SHELL 3**, as it will be shown in the next section for the other analyzed cantilever shapes.

The difference between the computed results and the experimental value of resonant frequency can be explained by execution errors of the structures – dimensional deviations, and, also, the value of the silicon elastic modulus considered in the computation, both analitic and numerical.

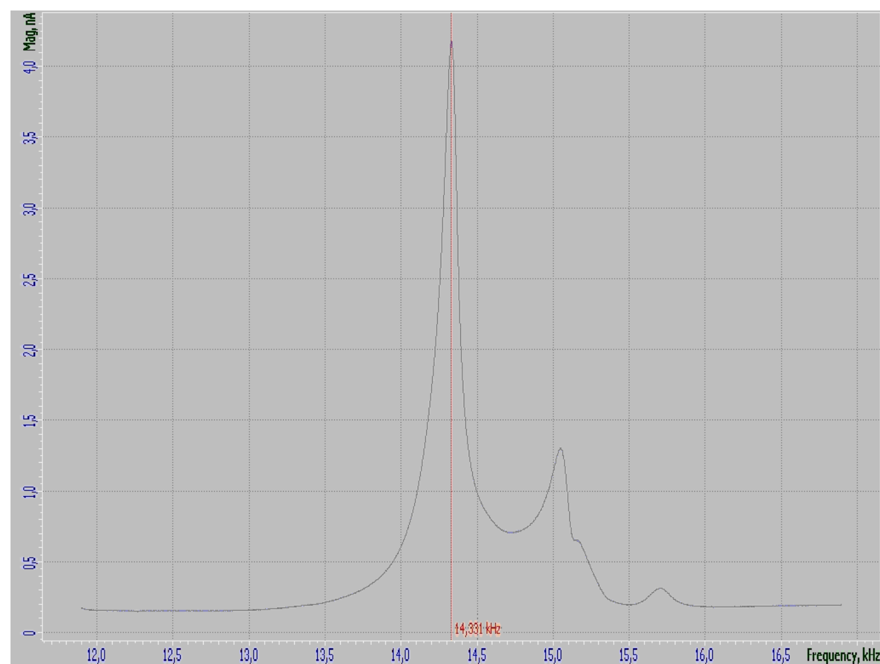

Fig. 4. Value of the first resonant frequency f_1 measured with the atomic force microscope.

It proceeded to the measurement of the beam sizes, and it found that the actual value of length is l_{real} = 727 μm, Fig. 5. The Nova NanoSEM 630 (FEI Company), an Ultra high Resolution Field Emission Scanning Electron Microscope (UhR FE-SEM), was used for measurements. According to Eqn. (1), the (l) length variations (23 μm) have an effect much more important than the (t) thickness variations (0.14 μm) on the resonant frequency, of over twice bigger (2.17 times); the third size, (b) width, does not appear in formula, because it simplifies in the I_y/A ratio. Using the numerical *model 2* of computation with l_{real}, it was obtained f_1 = 11.466 kHz, much different, yet, related to the experimentally determined value (Table 2) of the fundamental resonant frequency. Consequently, it has been necessary to measure the Young's modulus of cantilever material (silicon). Nanoindentation, applied on the Nano Indenter G200 (Agilent Technologies) equipped with CSM (Continuous Stiffness Measurement) module, was used.

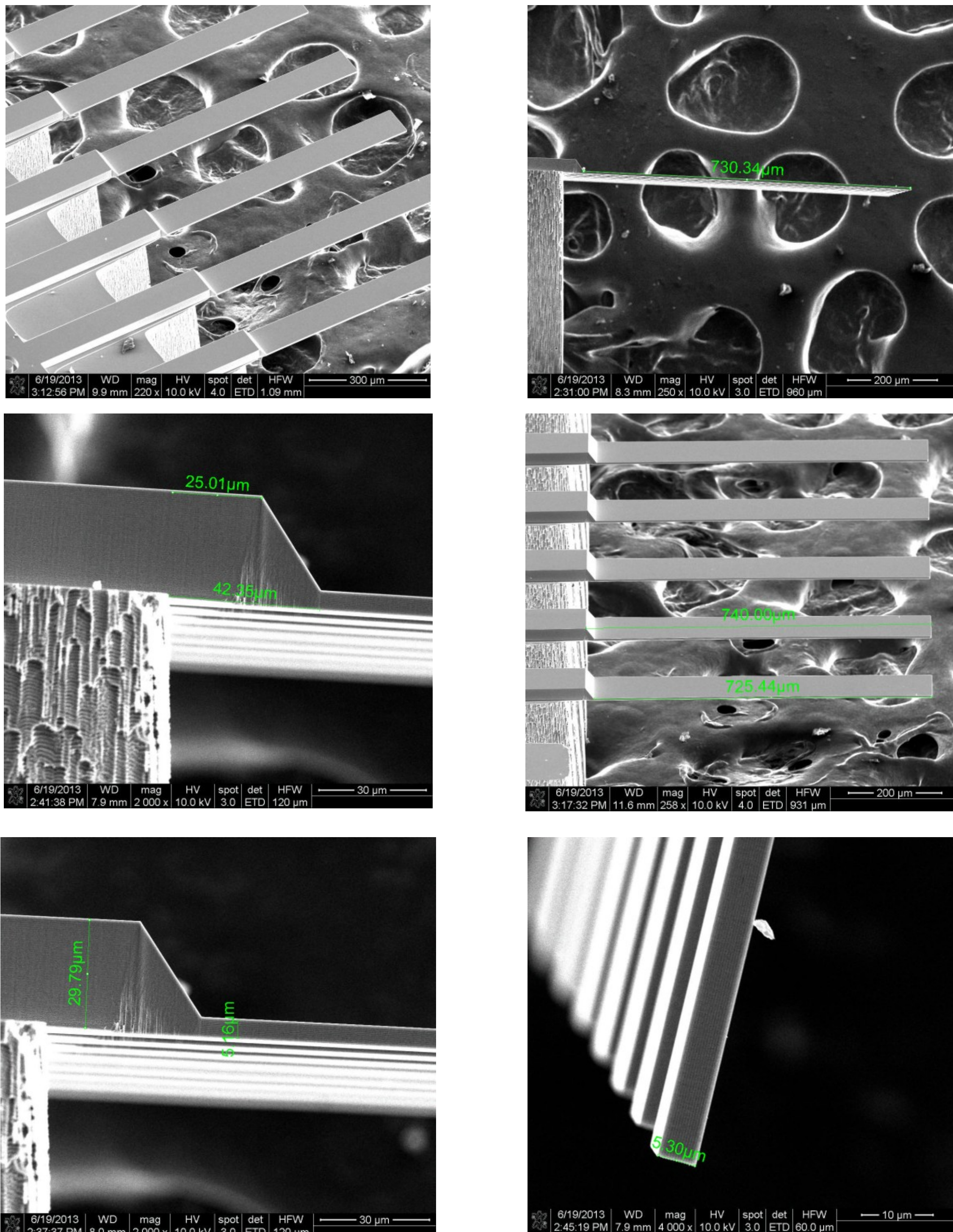

Fig. 5. SEM images of the rectangular microcantilevers.

The mechanical behaviour of the materials is described in terms of force per unit cross-sectional area, or stress (σ), and relative displacement per unit distance, or strain (ε). At low enough values of applied stress, the stress – strain relation of many solids is nearly linear and independent of time [17].

According to Fig. 6, the slope of the stress – strain curve in the elastic regime represents Young's modulus of elasticity, *E*. The yield strength, *Y*, is defined as the stress required to produce some specified plastic deformations, usually 0.2%. The value of the maximum load divided by the original area of the test sample is called ultimate tensile strength (*UTS* or σ_u). The value of the maximum stress required to break (or fracture) the test sample is called the tensile strength at the break, the breaking strength (*BS* or σ_b), or the fracture strength (σ_f).

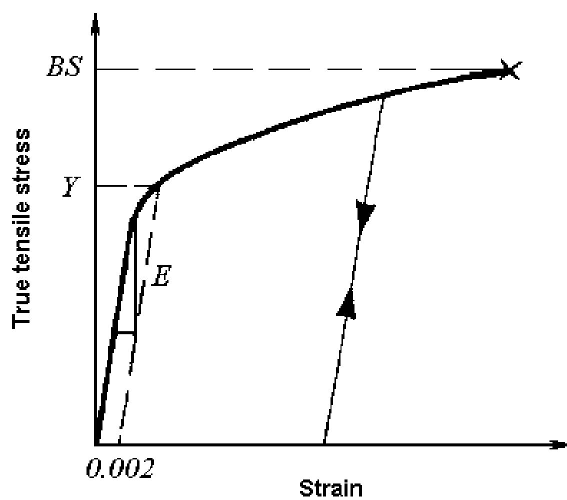

Fig. 6. Stress – strain curve for real solids – principle sketch.

The elastic properties of bulk solids with a high elastic modulus, such as metals and ceramics (and silicon, too), are generally measured with a tensile test machine. In our work, we have used the nanoidentation method as technique of elastic modulus measurement. The instrumented indentation testing (IIT) or depth sensing indentation (DSI) testing has become an alternative technique for determining the mechanical properties of materials on micro- and nanoscale, employing a nanoidentation apparatus. The method was introduced in 1992, and refined sometime later, in 2004, by W.C. Oliver and G.M. Pharr [18]. IIT is similar to a hardness test in that a rigid probe is pushed into the surface of a material. Traditional hardness tests return one value of hardness at a single penetration depth or force and for most techniques the computation of this single valued measurement requires that the area of the residual hardness impression to be measured optically, on a microscope.

IIT is an improvement to traditional methods because there is no need to measure the area of the residual impression. With instrumented indentation testing the area of contact is computed from the load-displacement history which is recorded continuously throughout the experiment. The slope of the unloading curve, which is always in the elastic range, is a measure of the elastic modulus.

The Young's modulus of silicon determined by nanoindentation with the Agilent Nano Indenter G200 is given in Fig. 7, and the computation values are listed in Table 3 (Young's modulus values and corresponding hardness values). It resulted E = 173.7 GPa. It was proved that the micromachining technology is mostly important

for the elastic constants of material, especially Young's modulus. For the presented case, the measured value of *E* was validated, being very close to that of the polysilicon, determined through traditional method with a tensile test machine [19].

Considering E = 173.7 GPa, b = 90 μm, t = 5 μm and l_{real}= 727 μm, the values of the first six eigen (natural) frequencies have been detemined, Table 4. The shape of the vibration modes with respect to the experimental ones, determined using MSA – 500, is given in Fig. 8.

It can be observed a very good concordance between the computed and measured values of the resonant frequency, for the „out-of plane" bending modes 1, 2, 4 and 6 (relative errors ≤ 1%). For the torsional mode 3, the relative error is of about 5.4% (computation *model 1*), respectively 6.9% (computation *model 2*). The mode 5 was not observed experimentally because it is a lateral mode („in plane"), and the micromechanical structures were excited in perpendicular direction on surface.

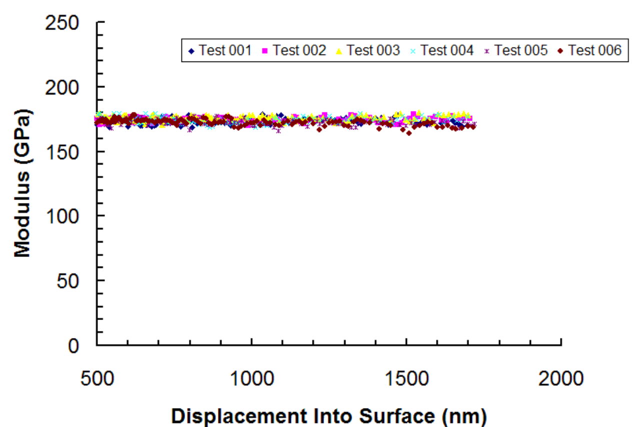

Fig. 7. Silicon Young's modulus determined by nanoindentation.

Table 3. Young's modulus values and corresponding hardness values.

Test	Average modulus [1000-1600 nm], GPa	Average hardness [1000-1600 nm], GPa
1	174.3	12.49
2	174.4	12.38
3	175.6	12.26
4	174.4	12.28
5	171.8	12.34
6	171.4	12.19
Mean	**173.7**	**12.32**

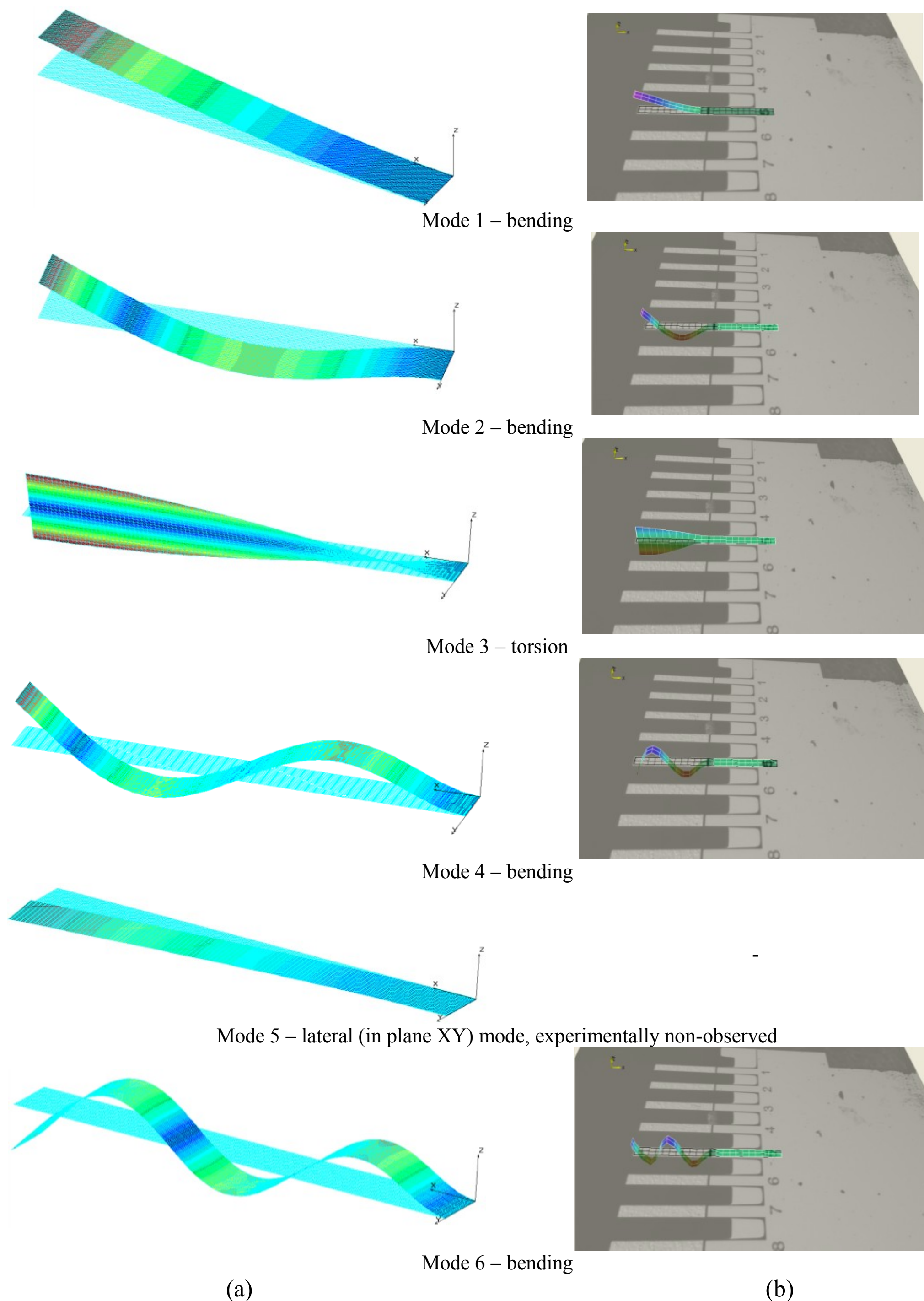

Fig. 8. Shape of the vibration modes, numerically (a) and experimentally (b) determined.

Table 4. Resonant frequency values, determined by computation and experimentally, and errors of the two models of computation related to the measured values.

Method \ Resonant frequency, kHz	f_1, bending mode	f_2, bending mode	f_3, torsion mode	f_4, bending mode	f_5, lateral mode	f_6, bending mode
FEM, *model 1* 3D SOLID	13.256	83.039	213.61	232.58	235.12	456.13
	0.18%	0.604%	5.382%	0.858%	-	1.186%
FEM, *model 2* SHELL 3	13.255	83.033	216.7	232.61	235.184	456.283
	0.188%	0.597%	6.906%	0.871%	-	1.22%
Experimental, MSA–500 (average values for the eight microbeams)	13.28	82.54	202.7	230.6	non-observed, in plane mode	450.78

As partial conclusions, it can be shown that precise results are obtained, by numerical computation, regarding both values of the eigen (natural) frequencies and shape of vibration modes, if the component sizes and, also, the value of the elastic modulus strongly depending on the crystalline structure of material and the used microfabrication technology (as the silicon case is), are exactly known.

Both models can be employed: **model 1** (3D FEM), for non-homogeneous, composite (multi – layer) structures and **model 2** (2D FEM) for homogeneous and thin structures, made from a single material (single – layer). The second model allows a lower effort of computation due to the reduced number of elements and nodes.

Another important conclusion refers to the deviation of about 19% between the measured value of resonant frequency and that one estimated by the producer for the reference chip. The specifications must be verified before utilization.

3. Natural frequencies of complex shape microcantilevers

n – (111) *silicon wafers* of 3 inch diameter and 375 µm thickness were thermally oxidized in wet oxygen atmosphere to obtain a silicon dioxide (SiO_2) layer of about 1.7 µm thickness, used both as protective layer (mask) during etching process, and as constructional material for cantilevers after releasing from substrate (the silicon wafer).

The oxide layer was photoengraved by means of a standard photolithographic technique, followed by etching in an HF – solution. Then, a similar method used for fabricating free-standing structures, as movable micromirrors or waveguides from microphotonic devices, was applied. In a first stage, in the opened windows, the silicon was plasma etched through a Bosch process using a DRIE (Deep Reactive Ion Etching) – Plasmalab System 100-ICP (Inductively Coupled Plasma) to a depth of about 40 µm. Two steps were performed: (1) a passivation process to 100 sccm flow rate of C_4F_3, and (2) an etching process to 100 sccm flow rate of SF_6; working pressure 10 mTorr at 15 °C, power in RF 5 W, ICP power 700 W and etch rate of 2 – 3 µm/min. So, on the silicon surface from the vertical walls of the etched cavities, the access to the faster etching (110) crystal planes was allowed in order to perform a second etching stage (wet etching), based on the anisotropy of silicon [20] .

Potassium hydroxide (KOH) 40% at 80 °C (lateral etch rate of about 100 µm/h along the <110> direction) was employed to release the SiO_2 cantilevers from the wafer surface. Two structures types were created: triangular – "V shaped" and inner-cut trapezoidal with rectangle tip cantilevers, as is shown in Fig. 9. The geometric parameters are given in Table 5. The areas of the two structures are the followings: $A_{triangular}$ = 5804.8 µm^2 and $A_{trapezoidal}$ = 7967.15 µm^2 (from which A_{tip} = 5174 µm^2). If the areas are divided to the lengths, assuming the cantilevers of rectangular shape, a width of about 38 µm results for both of them. So, it can observe that the triangular cantilever (L = 150.3 µm) is a stiff structure, while the trapezoidal cantilever (L = 204.4 µm) is a flexible structure.

For the complex shape cantilevers there are not analytical expressions to compute the eigen (natural) frequencies. Their estimation can be made only numerically with FEM. Because they are homogeneous structures (fabricated from a single material), model 2 SHELL 3, previously validated, was used: 4,062 elements interconnected in 2,203 nodes have resulted for the triangular form and, respectively, 7,252 elements interconnected in 3,881 nodes for the trapezoidal form.

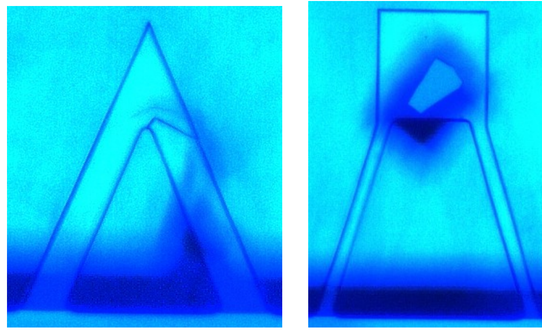

Fig. 9. Images (on optical microscope) of complex shape cantilevers made from SiO_2 layer (1.7 µm thickness) after release by etching the substrate (silicon wafer).

Table 5. Geometric parameters of the cantilevers.

Cantilever types and sizes (µm)	L	l	B	b	w	t (thickness)
	150.3	106	152	-	23	1.7
	204.4	134	151	73.5	10.5	1.7

The oxide layer was modeled as an isotropic material, with E_{SiO2} = 70 GPa, ν_{SiO2} = 0.17 and ρ_{SiO2} = 2200 kg/m^3 [21]. The shape of the simulated vibration modes is shown in Fig. 10, and the first five eigen (natural) frequencies computed with FEM are presented in Table 6.

The most close values to the experimental ones were obtained for a round – inner corner radius of 2 µm. As it was expected, for the stiffer structure, the triangular one, resonant frequencies higher, in (kHz – MHz) range, than for the trapezoidal cantilever have resulted. Fig. 11 demonstrates geometry and 3D motion of the microcantilevers at the first (fundamental) vibration mode viewed on MSA–500: $f_{1triangular}$ = 83.13 kHz, $f_{1trapezoidal}$ = 22.50 kHz.

A good agreement was obtained between experimental and computed frequencies: a relative error of 1.4% for the triangular cantilever and of 4.6% for the trapezoidal one.

Table 6. Resonant frequency values, determined by FEM computation.

Method / Cantilever type \ Resonant frequency, kHz		f_1, bending mode	f_2, combined (torsion + bending) mode	f_3, bending mode	f_4, combined (torsion + bending mode	f_5, bending mode
FEM, *model 2* SHELL 3	*triangular*	84.32	429.933	469.839	1137.17	1187.12
	trapezoidal	21.457	148.846	186.183	459.616	562.089

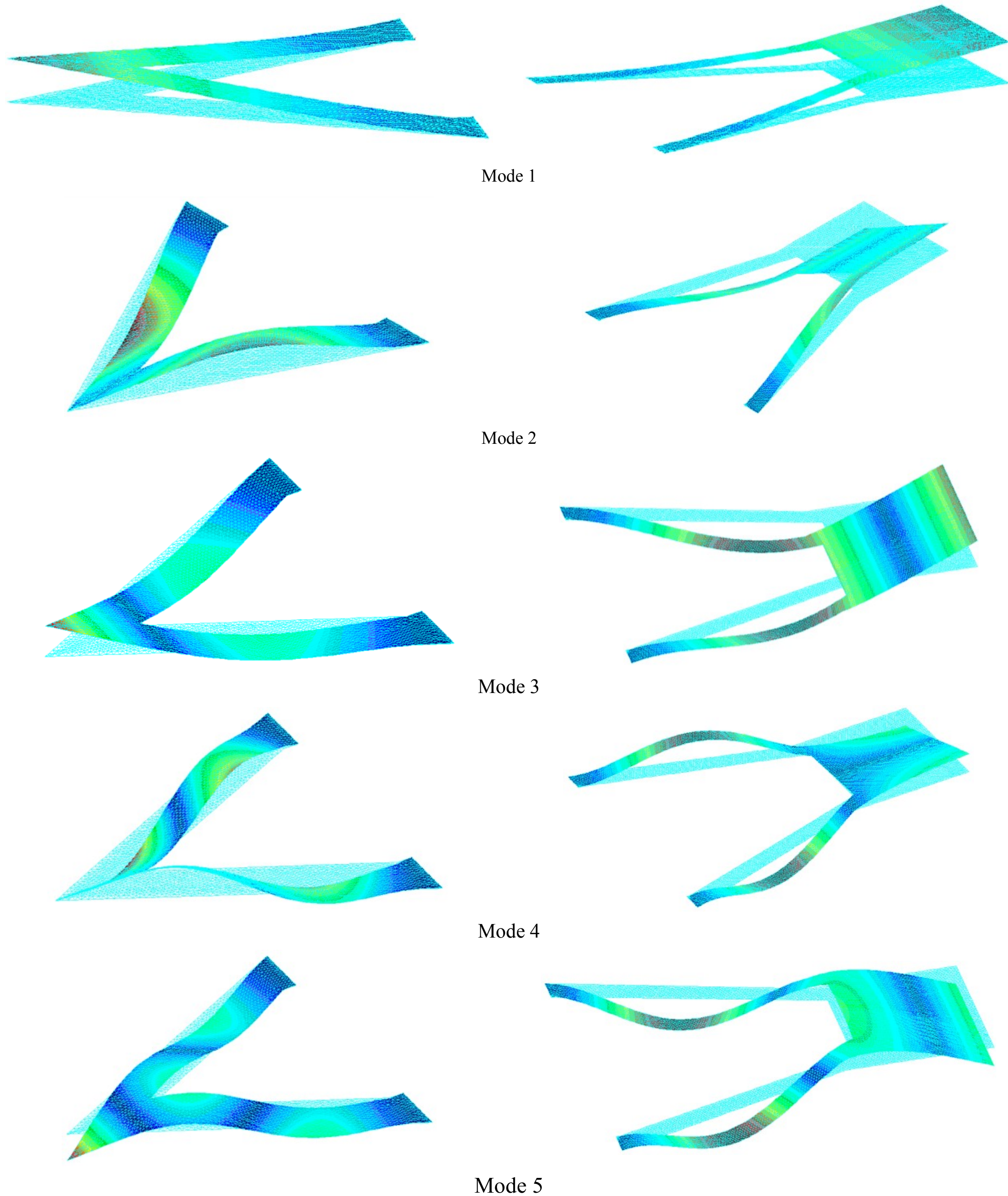

(a) *(b)*

Fig. 10. Shape of the numerically determined vibration modes for triangular – "V shaped" (a) and inner-cut trapezoidal with rectangle tip (b) cantilevers.

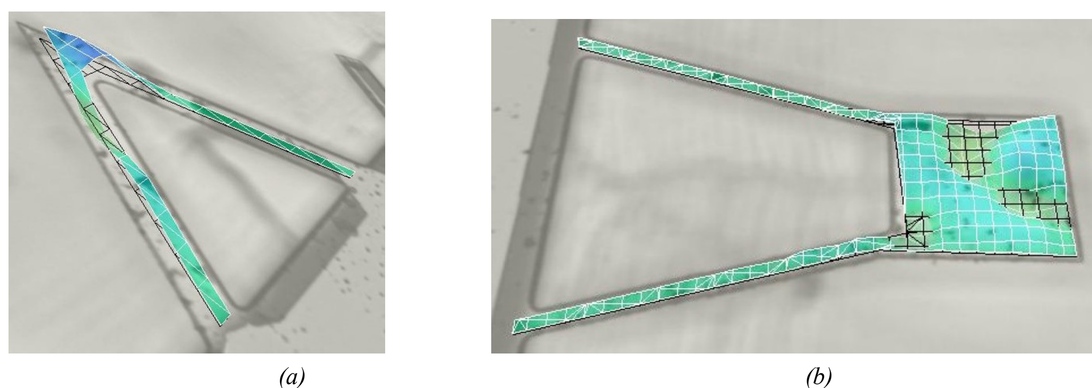

(a) (b)

Fig. 11. 3D motion of triangular (a) and trapezoidal (b) microcantilevers at the first (fundamental) vibration mode viewed on MSA–500.

4. Natural frequencies and sensitivity estimation of complex shape coated microcantilevers

The use of the two cantilevers of complex shape as sensitive elements of a chemical sensor for gas (hydrogen) detection has been simulated. Resonant detection methods rely on the change of the sensing system mass (by attachment of extraneous matter) or on the combined modification of mass and stiffness (as the case is of a layer – like deposition), which produces a variation in the fundamental resonant frequency. The element palladium (Pd) was selected as the absorbent layer for the cantilever because of its sensitivity to hydrogen. It has an ability to absorb (not adsorb) great quantities of hydrogen. A true benefit of this interaction is that the absorption can be occured at room temperature. The hydrogen then desorbs out of the palladium when the hydrogen source is removed. The one fact that limits hydrogen use is its explosive nature. Hydrogen is explosive from 4% to 40% concentration. The possibility to detect lower concentration limits (<<1% hydrogen) is studied. For this aim, the cantilevers are coated with a titanium (Ti) very thin film, of 10 Å (0.001 μm) thickness as an adhesive layer between the silicon-oxide and the palladium. The thickness of the Pd layer is 1000 Å (0.1 μm).

The two layers are deposited on the entire surface of the triangular cantilever and only on the rectangular tip surface of the trapezoidal cantilever (structure with concentrated mass to the end). The properties of materials are given in Table 7. The resonant frequencies computation was made employing the model 1 (3D SOLID), recommended for non-homogeneous (composite) structures.

It was assumed that the properties of the layers (including the silicon-oxide substrate) are isotropic in nature. The resonant frequency values are presented in Table 8 comparatively with those computed using the same model for the homogeneous (SiO_2) structures. The shapes of the eigen vibration modes are identical with those presented in Fig. 10.

Table 7. Properties of the used materials.

Material	Pd	Ti	SiO_2
Thickness, μm	0.1	0.001	1.7
Density, kg/m^3	12023	4507	2200
Young’s modulus, GPa	121	116	70
Poisson’s ratio	0.39	0.32	0.17

Table 8. Resonant frequency values, computed with model 1 (3D FEM) for homogeneous (SiO_2) and non-homogeneous (SiO_2-Ti-Pd) structures.

Method / Cantilever type		Resonant frequency, kHz: f_1	f_2	f_3	f_4	f_5
FEM, *model 1* 3 D SOLID	SiO_2 *triangular*	84.32	426.94	468.14	1131.47	1186.5
	non-homogeneous *triangular*	84.4	425.5	469.37	1130.32	1194.89
	SiO_2 *trapezoidal*	21.38	145.56	185.76	457.21	560.43
	non-homogeneous *trapezoidal*	18.74	134.00	177.16	462.88	558.52

Comparing the resonant frequencies of uncoated and coated cantilevers (Table 8), frequency shifts of (0.1÷0.34) % for the coated triangular cantilever and, of (0.34÷12.35) % for the coated trapezoidal cantilever can be observed. For the given dimensions and the coating manner, it is proved once more the stiffer behaviour of the triangular structure with respect to the trapezoidal one.

So, the sensitivity of the cantilevers, or their ability to detect frequency shifts due to absorption of the chemical target, was estimated. The sensitivity S, which represents the frequency variation per unit of added mass by absorption, can be calculated as:

$$S = \frac{\Delta}{\Delta} \quad (4)$$

Using FEM, the values of the frequency shift as a function of the deposited layer thickness variation (converted into added mass) were determined (Table 9). The „minus" sign shows a decrease of frequency.

The equivalent amount of mass of hydrogen accumulated on the cantilever by absorption can be calculated with the following equation [22]:

Δm H_2= (absorption_multiplier)(ρ H_2)(volume_Pd), (5)

where: absorption_multiplier is the conversion of the atomic ratio into the equivalent volume (~$1.25 \cdot 10^3$ cm^3H_2/cm^3Pd for a concentration of 1% H_2 in Pd at 20°C); ρ H_2 (8.3854 g/m^3) is the density of hydrogen determined for the specified conditions of partial pressure and temperature; volume_Pd (the coating area multiplied with Δt_Pd) is the palladium coating layer volume, which although changes with the absorption process, it does not increase in the overall volume mass (number of palladium molecules).

It is important to note that the partial pressure is of the gas to be detected from a sample of a gaseous mixture (for a concentration of 1% H_2, its partial pressure is of 0.01 atm in a mixture with nitrogen – the total pressure 1 atm).

Figures 12 and 13 present the frequency shifts for the first five vibration modes of the two cantilever types, triangular and trapezoidal, respectively.

In Fig. 14, a comparison between the two cantilevers is given, for the fundamental frequency shift. The range of the absorbed mass is similar for the two structures, of picograms order, but the frequency shifts of the trapezoidal cantilever are much more than for the triangular one (values higher with a magnitude order at least).

The slope of the curves gives us the sensitivity of the modified cantilevers: ~272 Hz/pg for the trapezoidal cantilever, and ~56 Hz/pg for the triangular one, estimated by trendlines.

Table 9. The simulated values of fundamental frequency shift as a function of Pd layer thickness variation converted in absorbed mass of hydrogen.

Δ*t*_Pd (μm)	Triangular cantilever		Trapezoidal cantilever	
	Δf_1 (Hz)	Δ*m* H_2 (pg)	Δf_1 (Hz)	Δ*m* H_2 (pg)
0.05	-37,50	3,042	-996,2	2,711
0.1	54,70	6,084	-1847,6	5,423
0.15	229,80	9,126	-2566,6	8,135
0.2	472,80	12,168	-3217,4	10,847

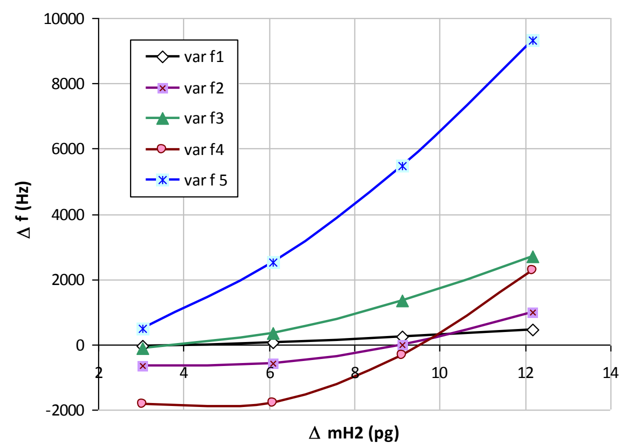

Fig. 12. The frequency variation for the first five vibration modes of triangular cantilevers as a function of the absorbed mass of hydrogen within the Pd layer.

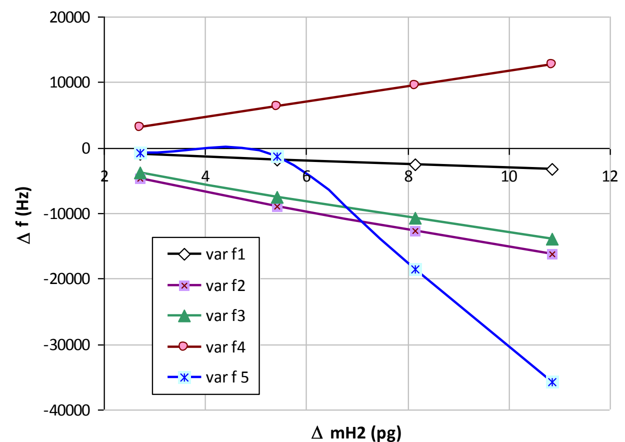

Fig. 13. The frequency variation for the first five vibration modes of trapezoidal cantilevers as a function of the absorbed mass of hydrogen within the Pd layer.

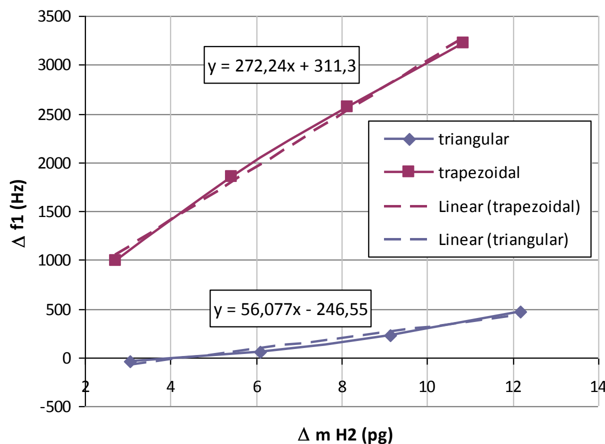

Fig. 14. The frequency variation for the first (fundamental) vibration mode of triangular and trapezoidal cantilevers as a function of the absorbed mass of hydrogen.

5. Conclusions

In this paper, a method of estimation by numerical simulation of the sensitivity of resonant non-homogeneous cantilevers with complex shapes has been proposed. The studied cantilevers are interesting in applications of biological and chemical sensors with high sensitivity (for instance, the flexible trapezoidal shape), as well as in atomic force microscopy (the stiff triangular shape) due to higher modes, useful for development of new imaging modes.

The LDV technique is an important tool to determine the resonant frequency of the cantilever structures, because it does not depend on the beam geometry or on an estimation of material properties.

However the FEM simulation and analytical computation (used in the case of the simplest configuration – rectangular cantilever) were useful to refine the range examined by LDV and in the preliminary design process, in order to validate the numerical computation models for the complex shape cantilevers.

The proposed models of computation with FEM, in order to estimate the dynamic behaviour and sensitivity of the studied microcantilevers, allow the change of geometrical parameters (shapes, thickness of layers, dimensions), and elastic properties (use of other materials, depending on the intended purpose and the micromachining technology of structures). Influence of the mentioned parameters on sensitivity opens new directions for future research regarding the optimization of these MEMS structures.

Acknowledgements

The MSA-500 testing system was acquired by the Politehnica University of Bucharest, National Mechatronics Centre, in the frame of Microlab project – The expansion of the capabilities of Computer Assisted Testing Laboratory for Mechatronics Systems in the micromechatronics field – project financed through the Capacities program, module 4.

References

[1] A. Raman, J. Melcher, R. Tung, Nanotoday **3**(1-2), 20 (2008).
[2] K. M. Goeders, J. S. Colton, L. A. Bottomley, Chem. Rev. **108**, 522 (2008).
[3] X. Liu, S. Cheng, H. Liu, S. Hu, D. Zhang, H. Ning, Sensors **12**, 9635 (2012).
[4] M. Stuchlik, P. Krecmer, S.R. Elliot, J Optoelectron Adv M **3**(2), 361 (2001).
[5] E. Finot, A. Passian, T. Thundat, Sensors **8**, 3497 (2008).
[6] G. Ionascu, C. D. Comeaga, L. Bogatu, A. Sandu, E. Manea, D. Besnea, J Optoelectron Adv M **13**(8), 998 (2011).
[7] I. R. Voiculescu, M. E. Zaghloul, R. A. McGill, E. J. Houser, J. F. Vignola, D. L. Jones, J Mech Eng Sci **220**, 1601 (2006).
[8] G. Louarn, S. Cuenot, Recent Advances in Modelling and Simulation, Giuseppe Petrone and Giuliano Cammarata (Eds.), 207-220 (Chapter 11), InTech, Vienna, Austria (2008).
[9] S. Subramanian, N. Gupta, J. Phys. D: Appl. Phys. **42,** 185501 (2009).
[10] H. Hocheng, W. H. Weng, J. H. Chang, Measurement **45**, 2081 (2012).
[11] L. Zhao, L. Xu, G. Zhang, Y. Zhao, X. Wang, Z. Liu, Z. Jiang, J Zhejiang Univ-Sci C (Comput & Electron) **14**(4), 274 (2013).
[12] M. Chaudhary, A. Gupta, Defense Science Journal **59**(6), 634 (2009).
[13] V. M. Reddy, G. V. S. Kumar, International Journal of Emerging Technology and Advanced Engineering **3**(3), 294 (2013).
[14] M. A. Hopcroft, W. D. Nix, T. W. Kenny, J. Microelectromech. S. **19**, 229 (2010).
[15] www.micromotive.de
[16] M. Rades, Mechanical Vibrations, vol. 1, Printech, Bucharest (2006).
[17] B. Bhushan, Tribology and Mechanics of Magnetic Storage Devices, Appendix A (Techniques for Measuring Mechanical Properties of Thin Films), Springer-Verlag New York Ink. (1990).
[18] W. C. Oliver, G. M. Pharr, J. Mater. Res. **19**(1), 3 (2004).
[19] W. N. Sharpe, Jr., Bin Juan, R. Vaidyanathan, Proc. 10-th IEEE Intern. Workshop on Microelectromechanical Systems, Nagoya, Japan, 1997, p. 424.
[20] D. Cristea, M. Purica, E. Manea, V. Avramescu, Sensors and Actuators A **99**, 92 (2002).
[21] S. V. Kamat, DRDO Science Spectrum, March, 203 (2009).
[22] D. Arreco, Analysis and Preliminary Characterization of a MEMS Cantilever-type Chemical Sensor, Center for Holographic Studies and Laser micro-mechaTronics (CHSLT), Mechanical Engineering Department, Worcester Polytechnic Institute (2003).

*Corresponding author: ionascu_georgeta@yahoo.com